On the describing functions for dampers with freeplay and dry friction for studying nonlinear oscillations

Breno M. Castro[a], Wellington L. Paulo Jr[a], Douglas D. Bueno[b], Paulo J. Paupitz Gonçalves[c]

[a]*EMBRAER - Technology Development Department, Av. Brigadeiro Faria Lima, 2170, São José dos Campos, 12.227-901, São Paulo, Brazil*
[b]*School of Engineering, Ilha Solteira (UNESP), Avenida Brasil, 56, Ilha Solteira, 15.385-007, São Paulo, Brazil*
[c]*School of Engineering, Bauru (UNESP), Av. Eng. Luiz Edmundo C. Coube, 14-01, Bauru, 17.033-360, São Paulo, Brazil*

Abstract

This work presents a novelty in the mathematical formulation of a damper with Freeplay for structural dynamics analysis in the frequency domain. This theoretical model represents the basis for the application of the harmonic balance technique for simulating problems with nonlinear characteristics. The predictions of the mathematical model proposed in this work are confronted with results obtained on a ground test of an apparatus composed of a damper and an attachment with a fixed amount of Freeplay. The results indicate that the proposed mathematical model can capture the nonlinear characteristics of a damper with Freeplay and, therefore, be used for nonlinear structural dynamics analyses, mainly focused on aeroelastic stability.

Keywords: damper, freeplay, combined concentrated nonlinearity, limit cycle oscillation prediction

1. Introduction

Oscillatory phenomena pose significant challenges for engineers and researchers involved in the design, manufacturing, and operation of various mechanical systems, particularly in the aerospace industry. These challenges are critical because they often result from interactions between the airflow around an aircraft and its structural components. Extensive research has

been dedicated to fluid-structure interaction problems, with a strong emphasis on the mathematical formulation of linear dynamic models. However, certain oscillatory behaviors that arise under specific flight or structural conditions cannot be adequately captured by linear models.

A particularly notable oscillatory phenomenon is Limit Cycle Oscillation (LCO), characterized by the gradual development of sustained oscillations with limited amplitude under specific operating conditions. Woolston et al. [1] were among the first to demonstrate that such oscillatory behavior in aeroelastic systems can result from nonlinear dynamics, potentially evolving into a catastrophic flutter that is self-limited and less violent. Despite this early recognition, developing representative nonlinear dynamic models and analysis methods for practical applications remains a challenging task.

LCOs are observed in different aeronautical systems, such as control surfaces, moving wings, external stores and landing gears [2, 3, 4]. They can accelerate structural fatigue and compromise aircraft controllability, resulting in dangerous flying conditions. Because of this, different authors have also contributed to develop effective controller design techniques for LCO suppression [5, 6].

One common source of LCO in aircraft control surface is the presence of freeplay in spring-type components within dynamic systems, and the oscillatory behavior is observed in different aerodynamic regimes [7, 8]. Freeplay is often verified in landing gears, control surface actuators, or engine-pylon attachments to wings, and it can induce periodic and aperiodic motions [9, 10]. Since freeplay is an inevitable consequence of manufacturing tolerances, it has become a critical area of study for aviation professionals, which is also considered important by aeronautical certification agencies, as reported by Panchal and Benaroya [11].

Although different authors have investigated aeroelastic systems with freeplay, the prediction of dynamic responses considering freeplay combined with another source of nonlinearity can require additional effort [11]. In this sense, Pereira and colleagues [12] studied the quadratic and cubic forms of nonlinear couplings due to the combined hardening and freeplay effects, whereas Eller [13] and Wayhs-Lopes et al. [14] evaluated the influence of friction and Freeplay on LCO. In addition, Kholodar [15] noted that a certain amount of aerodynamic preload on the control surface with freeplay can induce higher frequency oscillation in comparison with an unloaded condition. In practice, this type of analysis for real structures typically requires simplified component representations (i.e., models) arranged to mimic the actual

structure, aiming for accurate behavior prediction. The components such as control-surface actuators, landing gears, or engine pylons are often idealized as interconnected springs, dampers, and concentrated masses.

The use of simplified mathematical models is an interesting alternative to evaluate oscillating systems with concentrated nonlinearity (i.e., in a relatively small region of space) [16]. Den Hartog [17] introduced very useful analytical models involving freeplay and friction, for example, and more recently, Padmanabhan [18] presented different describing-function-based models involving stiffness and damping in terms of polynomial and freeplay. The author's model type named 'Freeplay damping' describes a linear viscous damper with freeplay, and this combination is previously investigated by Tong and Liebner [19], focused on evaluating energy dissipation. Note that a control surface actuator in failure mode can exhibit an equivalent damping behavior [20]. However, important aspects on the use of a mathematical model combining damper and freeplay remain less explored in the literature.

The flight control surfaces of modern aircraft are typically operated by hydraulic actuators. The control actuator is connected to the moving part via a link mechanism, as illustrated in a schematic drawing shown in Fig. 1. Considering that regulatory agencies of aircraft generally permit small freeplay tolerances within these connections, if an equivalent damping behavior is verified, the corresponding two force diagrams are displayed for a freeplay of dimension 2δ when the system is subject to displacement (x) with amplitude varying in the interval $[-A, A]$ (or, conversely, with an amplitude A).

The diagram shown in Fig.1(a) illustrates a spring with freeplay, and Fig.1(b) depicts a viscous damper with freeplay. The force diagrams for each case differ significantly from each other. The forces for the spring are zero around the central equilibrium position, whereas for the damper, they drop to zero at the minimum and maximum displacements of the actuator. Based on these schematic representations, the present article proposes an approach to evaluate a damper-freeplay combination. The damper with freeplay idealization introduced by Tong and Liebner [19] is considered. The novelty herein is a describing function obtained from a strategy based on the Harmonic Balance Method (HBM). It is presented in terms of freeplay, damping coefficient and both frequency and amplitude of motion. A second version of this describing function is derived when considering the friction effect. They are convenient models for aeroelastic analysis simultaneously including the effects of equivalent damping, friction and freeplay, typically observed in control surface actuator in failure modes. The model's accuracy is demon-

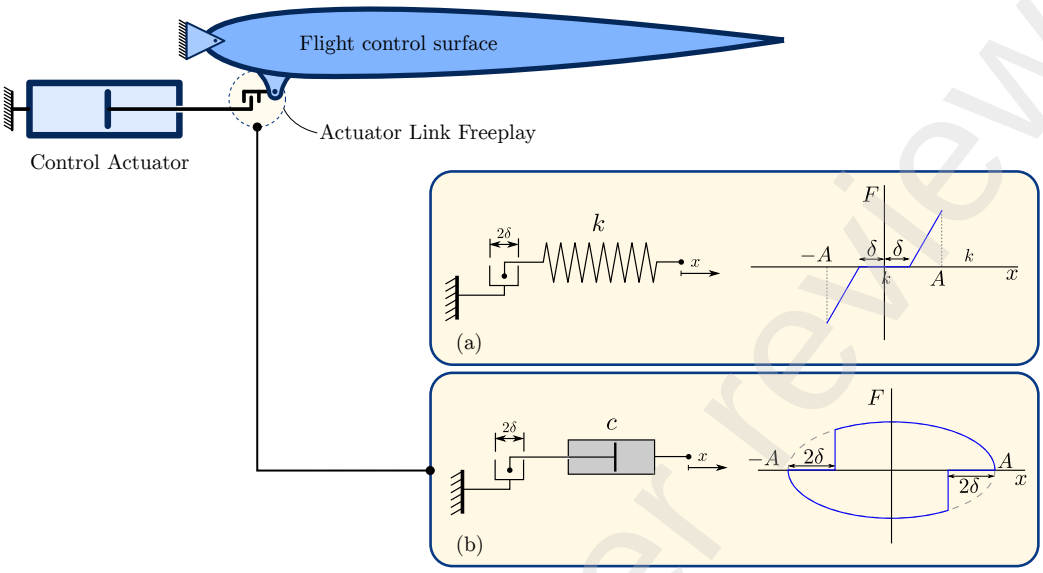

Figure 1: A flight control surface controlled by an actuator with a Freeplay 2δ in its link connections. (a) A spring subject to Freeplay and its force diagram, (b) a damper with Freeplay an its force diagram. Amplitude of motion is A.

strated by comparing theoretical predictions with experimental data from actual damper-freeplay systems.

The significance of this work lies in the need to establish safety criteria concerning the occurrence of flutter and related phenomena. Specifically, the Advisory Circular AC23-629-1B, issued by the FAA, addresses flutter conditions, with particular emphasis on cases involving Freeplay in aircraft control surfaces [21]. While Freeplay is typically associated with elastic elements (stiffness), in the event of a hydraulic system failure, the control surface actuator behaves as a hydraulic damper [20].

Considering that most existing studies focus on modeling Freeplay in stiffness elements, this work aims to investigate the problem of Freeplay in the context of hydraulic actuator failure. An approximate model is proposed based on the HBM using a describing function to account for Freeplay in a damper. Two cases are presented: the first one considers a linear viscous damper with Freeplay, and the second examines the same damper with Freeplay but in the presence of Coulomb friction.

The article is organized in four sections, including this introduction. The second section describes the methodology for modeling Freeplay on spring

and dampers. The third section shows experimental procedure to validate the model developed on section 2. Finally section four presents discussion and conclusions. An appendix shows methodology to obtain describing functions for dampers with Freeplay.

2. Harmonic Balance Method and Describing Functions

The Harmonic Balance is a method used to approximate periodic solutions of nonlinear differential equations. It is based on the assumption that the response of a nonlinear system to a periodic input can be expressed as a sum of harmonic (sinusoidal) components. The goal is to balance the harmonics (typically up to a certain number) of the nonlinear system's response with those of the forcing function [22].

The Describing Function (DF) is used in the analysis of nonlinear systems, particularly for studying stability and predicting limit cycles. It is most commonly applied in systems with nonlinearities like saturation, dead zones, relays and Freeplay, where exact solutions are difficult to obtain. The describing function is essentially a frequency-dependent gain and phase shift that approximates the effect of a nonlinearity on a sinusoidal input. The gain and phase shift can usually be obtained from the amplitude of the fundamental frequency obtained from the HBM. In summary, the DF is a linearization of a nonlinear element subjected to a sinusoidal input [23, 22] and it can be represented by a Frequency Response Function, Eq. (1), of an equivalent linear system.

$$H_{\text{eq}}(\omega) = \frac{1}{-m_{\text{eq}}\omega^2 + \mathrm{i}c_{\text{eq}}\omega + k_{\text{eq}}} \tag{1}$$

where, m_{eq} is the equivalent mass, c_{eq} is the equivalent viscous damper coefficient and k_{eq} is the equivalent stiffness, i is the imaginary unity, and ω is the circular frequency. Each equivalent parameter can be defined using the first order approximation for the Fourier series. One example is the case of a spring with a freeplay, where the force-displacement diagram is shown in Fig. 1(a). Using the procedure described in the Appendix, it is possible to obtain the equivalent stiffness expression based on the size of the freeplay (δ) and the nominal stiffness (k) as:

$$(k_{\text{eq}})_{\text{stiffness with freeplay}} = k\left[1 - \frac{2}{\pi}\arcsin\left(\frac{\delta}{A}\right) - \frac{2}{\pi}\left(\frac{\delta}{A}\right)\sqrt{1-\left(\frac{\delta}{A}\right)^2}\right] \tag{2}$$

2.1. Damping Freeplay (case 1)

In the same fashion, when the system under investigation has a damper with Freeplay (or a damping equivalent behavior with freeplay) in one of its connections with other parts of the dynamic system, the damping coefficient of this component is subject to variations as a function of the length of the deadspace region and of the motion characteristics such as amplitude and frequency.

In order to obtain a describing function for the damper with Freeplay, in a similar approach to what has been done to the spring with Freeplay, it is necessary to adopt a model to the nonlinear behavior of such a characteristic of the system, similarly to the idealization represented in Fig. 1(a). The starting point is a damper in which the damping force generated when it is not in the Freeplay region can be considered as linear and, consequently, proportional to the displacement velocity, such as $F(t) = c\,\dot{x}(t) = cA\omega\cos(\omega t)$, where c is the damping coefficient.

It is assumed that the presence of Freeplay can only be perceived when the force developed by the damper goes to zero and switches sign, i.e., from the moment that the end of the damper arm reaches its point of maximum displacement (see Fig.1(b)).

From this moment, due to the Freeplay, the end of the damper's arm moves without transferring any force to the system and only regains this force transferring condition when it reaches the limit of the Freeplay region, already with a velocity different from zero. Therefore, there is a discontinuity in the transferring of the force developed by the damper, which now becomes proportional again to the displacement velocity of the damper's arm.

The mathematical model proposed in this work is conceptually different from previous studies as the latter treats damping Freeplay with the same nonlinear idealization developed and used for stiffness Freeplay (see, for instance, Ref. [18]). It consists of a direct substitution of the displacement, x, by the displacement velocity, $\dot{x}$, in the behavior described in Fig. 1(a).

One detail on the model of Fig. 2(a) is that the limits of the Freeplay deadspace are not immediately identifiable, since they are dependent on the oscillation frequency. Note that this feature can present a challenge in terms of time domain simulations. However, for the frequency domain analysis, the ratio $\omega\delta/\omega A$ is equivalent to δ/A and, therefore, Eq. (2) can be used as it is, just switching k_{eq} for c_{eq} and k for c.

The difference of the present model is that the behavior of the force, $F(\dot{x})$, with respect to the velocity, $\dot{x}$, is the one illustrated in Fig. 2(a). The nonlin-

ear behavior is identified, in the figure, by the orange arrows indicating the path of the damping force throughout one cycle of the harmonic oscillation. Note that the path in one direction is different from the other's and also that there is a discontinuity in the force when the damper displacement is at the end of the Freeplay region. In terms of the force-velocity diagram, the amount of Freeplay in terms of velocity is defined by $2\omega\sqrt{A\delta - \delta^2}$.

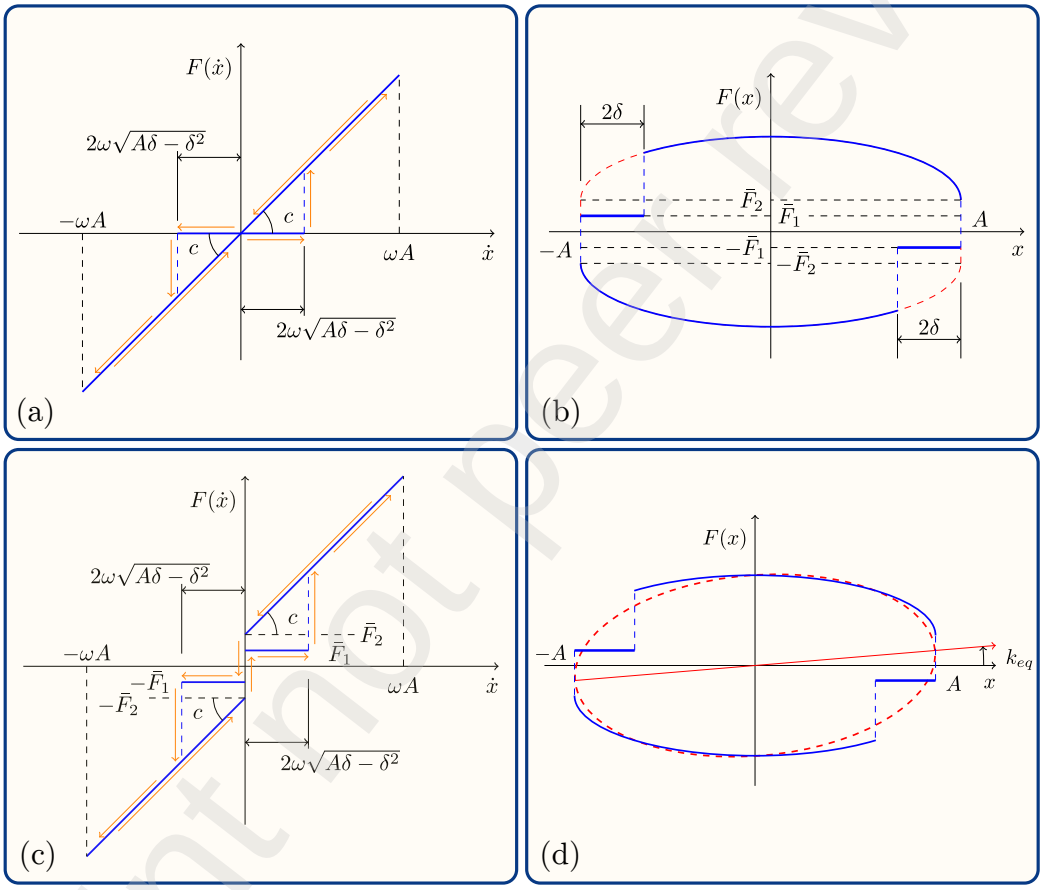

Figure 2: Idealization of the nonlinear behavior of a damper with Freeplay. (a) Force-velocity diagram of a damper with Freeplay. (b) Force-Displacement diagram of a damper with Freeplay and Coulomb Friction. (c) Force-Velocity diagram of a damper with Freeplay and Coulomb Friction. (d) Force-displacement diagram of the equivalent damper with freeplay.

Using the methodology described in the appendix (see also [22, 23]), the expansion of the idealized force in a Fourier series, truncating on the first

harmonic, leads to a description of the force developed by the damper with Freeplay given by Eq. (3).

$$\begin{aligned} F(t) &= \frac{c}{\pi}\left\{\pi - \arccos\left(1-\frac{2\delta}{A}\right) + \left(1-\frac{2\delta}{A}\right)\sqrt{1-\left(1-\frac{2\delta}{A}\right)^2}\right\}\dot{x}(t) \\ &\quad + \frac{c\omega}{\pi}\left[1-\left(1-\frac{2\delta}{A}\right)^2\right]x(t) + \text{H.O.T.} \end{aligned} \tag{3}$$

A simple inspection of Eq. (3) shows that the presence of Freeplay in the connection of a damper with other components (which, in case of absence of Freeplay, is linear) induces the appearance of an extra term that is proportional to the damper's displacement and not only to its velocity. Therefore, one notices that the presence of Freeplay induces a term with stiffness like characteristics (force in phase with the displacement). It is, then, an equivalent stiffness, induced by the presence of Freeplay, and not an actual or physical stiffness of the damper. Furthermore, it can be seen that the equivalent damping depends only on the size of the Freeplay zone and on the amplitude of the displacement, while the equivalent stiffness depends also on the frequency of motion. Hence, it is possible to separate Eq. (3) into a damping like component and another related to the equivalent stiffness of the damper with Freeplay:

$$(c_{\text{eq}})_{\text{case 1}} = \frac{c}{\pi}\left\{\pi - \arccos\left(1-\frac{2\delta}{A}\right) + \left(1-\frac{2\delta}{A}\right)\sqrt{1-\left(1-\frac{2\delta}{A}\right)^2}\right\} \tag{4}$$

$$(k_{\text{eq}})_{\text{case 1}} = \frac{c\omega}{\pi}\left[1-\left(1-\frac{2\delta}{A}\right)^2\right] \tag{5}$$

It is noticeable from Eqs. (4) and (5) that the equivalent damping coefficient is not affected by the frequency, only by the values of amplitude and size of the Freeplay zone. This is expected since the damping coefficient assumed to exist outside the deadspace is of a linear type, i.e., independent of the frequency. However, considering the case of the equivalent stiffness, there is influence from size of Freeplay as well as from frequency and amplitude of the displacement. The force-displacement diagram of a linear viscous

damper has an elliptical shape. In the case of the damper with damper with Freeplay, this the ellipse has an slope, with respect to the x-axis, as it can be seen in Fig. 2(d). The tangent of the inclination angle is related to the equivalent stiffness given by Eq. (8).

2.2. Damping Freeplay with Coulomb Friction (case 2)

Another source of nonlinear behavior is friction. The existence of friction forces between moving parts of a damper can also contribute to the overall damping of this component in a dynamic system. And similarly to Freeplay, friction is also inevitable in a mechanical system when there is contact between moving parts as in a damper. A way of modeling the friction force is by the assuming Coulomb Friction:

$$F_{\text{fr}} = \bar{F}\,\text{sgn}(\dot{x}) \tag{6}$$

in which $\bar{F}$ corresponds to the magnitude of the friction force and sgn( ) is the sign function. The friction force direction, though, is always opposite to motion's.

Coulomb friction force is already a source of nonlinearity, which is then combined with the nonlinearity due to the Freeplay region. These corresponding two forces are described considering that case in which the friction inside the damper is given by $\bar{F}_2$ and in the region of the Freeplay zone it is given by $\bar{F}_1$. It seems reasonable to consider that these two levels of friction are different each other because they come from different sources. The idealization of the behavior of a component with these characteristics is introduced in the Force-Displacement diagram shown in Fig. 2(b).

Considering the conditions of a viscous damper and the description of the friction force in Eq. (6) with the nonlinear behavior presented in Fig. 2(c), the following equations are obtained for the values of equivalent damping and stiffness for the nonlinear damper with friction in the damper itself and also in the Freeplay region.

$$\begin{aligned}(c_{\text{eq}})_{\text{case 2}} &= \frac{c}{\pi}\left\{\pi - \arccos\left(1-\frac{2\delta}{A}\right) + \left(1-\frac{2\delta}{A}\right)\sqrt{1-\left(1-\frac{2\delta}{A}\right)^2}\right\} \\ &+\frac{2(\bar{F}_2+\bar{F}_1)}{\pi A\omega} + \frac{2(\bar{F}_2-\bar{F}_1)}{\pi A\omega}\left(1-\frac{2\delta}{A}\right)\end{aligned} \tag{7}$$

$$(k_{\text{eq}})_{\text{case 2}} = \frac{c\omega}{\pi}\left[1-\left(1-\frac{2\delta}{A}\right)^2\right] + \frac{2(\bar{F}_2-\bar{F}_1)}{\pi A}\sqrt{1-\left(1-\frac{2\delta}{A}\right)^2} \quad (8)$$

It can be noticed that one of the effects of introducing friction in the damper with Freeplay, in light of Eqs. (7) and (8), is that the damping becomes influenced by the motion frequency, in contrast to the prediction of the model without friction. For low frequencies, the damping is dominated by the friction contribution. Nonetheless, the effect of the friction force tends to vanish for high frequencies and the damping tends to a constant value with respect to the frequency of motion.

3. Experimental Validation

Experimental tests were conducted on a dynamic test machine to demonstrate the methodology and validate the proposed models. The tests were performed using an MTS Test Machine, model 647, equipped with Hydraulic Wedge Grips. A force transducer, MTS model 661.20H-03, with a capacity of measuring up to 100 kN, was employed. Data acquisition was handled by a computer running MTS FlexTest 40 software, which recorded force and displacement values.

The test specimen was a LU JIN model LJ400AX dry damper, where the damping medium is air. The damper was connected to a mechanism designed to simulate Freeplay in the motion, as depicted in Fig. 3(d). Data was acquire using a sampling rate of 1024 Hz.

A sinusoidal displacement was applied to one end of the damper, with tests conducted at three different amplitudes and three different frequencies. The Freeplay was kept constant for all test runs, with a value of $2\delta = 0.0013$ m.

Figures 3(a), 3(b) and 3(c) present the curves measured in tests with amplitudes of $A = 1.0$ mm, $A = 2.5$ mm, and $A = 4.0$ mm, respectively. Each graph corresponds to three oscillation frequencies of the nonlinear damper: $f = 1.0$ Hz, $f = 3.0$ Hz and $f = 5.0$ Hz. It can be observed that the curves describing the force as a function of the relative displacement x of the damper ends resemble the idealized model and depicted in Fig. 2(b).

The consistence of the mathematical model under investigation in relation to the experimental results was verified by extracting the values of equivalent

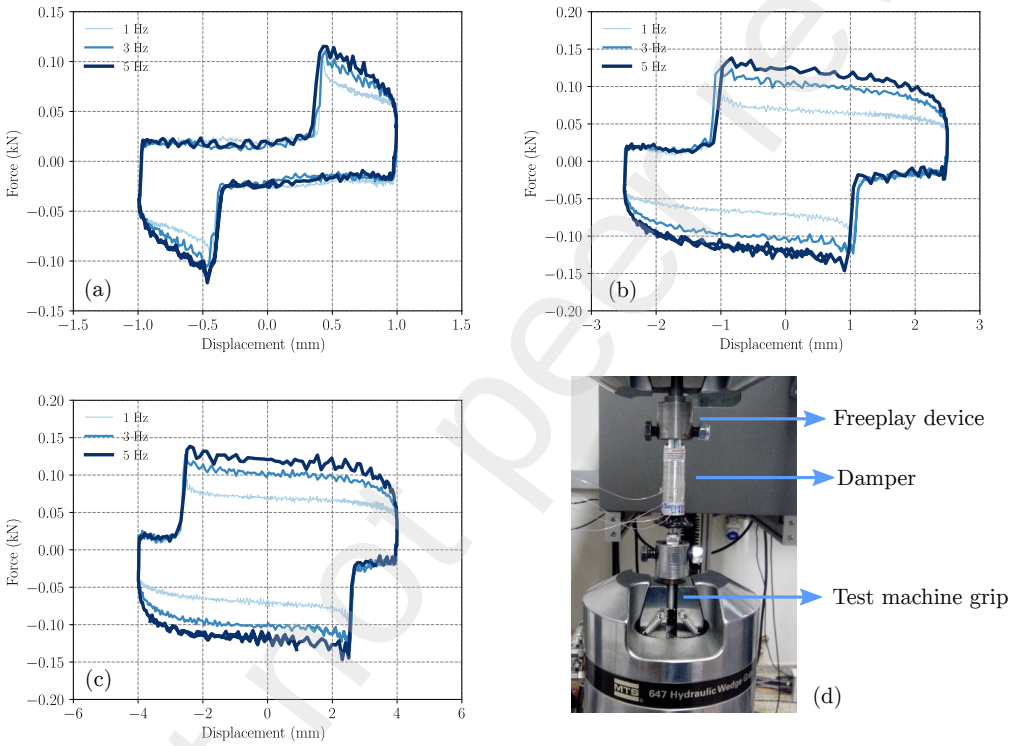

Figure 3: Experimental test results for different frequencies of excitation: (a) Force results for amplitude of 1 mm. (b) Force results for amplitude of 2.5 mm. (c) Force results for amplitude of 4 mm. (d) Detail of the experiment with damper and Freeplay device.

stiffness and damping from the measured according to the following equations.

$$k(\omega_1) = \mathrm{Re}\left\{\frac{\mathcal{F}[F(t)]_{\omega=\omega_1}}{\mathcal{F}[x(t)]_{\omega=\omega_1}}\right\} \qquad c(\omega_1) = \frac{1}{\omega_1}\,\mathrm{Im}\left\{\frac{\mathcal{F}[F(t)]_{\omega=\omega_1}}{\mathcal{F}[x(t)]_{\omega=\omega_1}}\right\} \tag{9}$$

where $\mathcal{F}[.]$ represents the Fourier Transform of a function, $F(t)$ is the force, and $x(t)$ describes the position, all described in the time domain.

After applying Eqs. (9), by using a Discrete Fourier Transform (DFT), the values of equivalent stiffness and damping were obtained, for a combination damper-Freeplay-friction, presented in Tab. 1.

Table 1: Values of equivalent stiffness and damping obtained from the experimental procedure.

Frequency (Hz)	Amplitude (mm)	Stiffness (N/m)	Damping (N.s/m)
1	1.0	32262.	7186.
	2.5	8854.	4253.
	4.0	3980.	3002.
3	1.0	38111.	2498.
	2.5	13023.	2026.
	4.0	6078.	1413.
5	1.0	41356.	1720.
	2.5	15926.	1359.
	4.0	7668.	964.

The evaluation of the mathematical model formulated for the damper with Freeplay and friction is done, then, by the comparison of values provided by the equations that describe stiffness and damping of the investigated model, Eqs. (7) and (8), with those obtained with the ground tests.

The computation of data for the damper with Freeplay and friction from data obtained in tests and represented in Tab. 1 can be done by using the Least Squares Method. The values for equivalent damping and stiffness can be respectively represented in the following manner:

$$\begin{aligned} c_{\mathrm{eq}} &= \alpha\, c + \beta\, \bar{F}_1 + \gamma\, \bar{F}_2 \\ k_{\mathrm{eq}} &= \eta\, c + \lambda\, \bar{F}_1 + \sigma\, \bar{F}_2 \end{aligned} \tag{10}$$

in which:

$$\alpha = \frac{1}{\pi}\left\{\pi - \arccos\left(1-\frac{2\delta}{A}\right) + \left(1-\frac{2\delta}{A}\right)\sqrt{1-\left(1-\frac{2\delta}{A}\right)^2}\right\}$$

$$\beta = \frac{2\delta}{\pi^2 A^2 f}$$

$$\gamma = \frac{1}{\pi^2 A f}\left(2-\frac{2\delta}{A}\right)$$

$$\eta = 2f\left[1-\left(1-\frac{2\delta}{A}\right)^2\right]$$

$$\lambda = -\frac{2}{\pi A}\sqrt{1-\left(1-\frac{2\delta}{A}\right)^2}$$

$$\sigma = \frac{2}{\pi A}\sqrt{1-\left(1-\frac{2\delta}{A}\right)^2}$$

where f is the frequency in Hertz and $\omega = 2\pi f$.

An error function, to be minimized, can be defined considering both the error in predicting the equivalent damping and the stiffness, in which n represents the number of test points and i refers to each point of the test.

$$E^2 = \sum_{i=1}^{n}\left[(\alpha_i\, c + \beta_i\, \bar{F}_1 + \gamma_i\, \bar{F}_2 - c_{\mathrm{eq},i})^2 + (\eta_i\, c + \lambda_i\, \bar{F}_1 + \sigma_i\, \bar{F}_2 - k_{\mathrm{eq},i})^2\right] \tag{11}$$

The minimization of the quadratic error defined in Eq. (11) leads to a system of equations described in:

$$\begin{cases} \sum_{i=1}^{n}(\alpha_i^2+\eta_i^2)c + \sum_{i=1}^{n}(\alpha_i\beta_i+\eta_i\lambda_i)\bar{F}_1 + \sum_{i=1}^{n}(\alpha_i\gamma_i+\eta_i\sigma_i)\bar{F}_2 = \sum_{i=1}^{n}(\alpha_i c_{\mathrm{eq},i}+\eta_i k_{\mathrm{eq},i}) \\ \sum_{i=1}^{n}(\beta_i\alpha_i+\lambda_i\eta_i)C + \sum_{i=1}^{n}(\beta_i^2+\lambda_i^2)\bar{F}_1 + \sum_{i=1}^{n}(\beta_i\gamma_i+\lambda_i\sigma_i)\bar{F}_2 = \sum_{i=1}^{n}(\beta_i c_{\mathrm{eq},i}+\lambda_i k_{\mathrm{eq},i}) \\ \sum_{i=1}^{n}(\gamma_i\alpha_i+\sigma_i\eta_i)c + \sum_{i=1}^{n}(\gamma_i\beta_i+\sigma_i\lambda_i)\bar{F}_1 + \sum_{i=1}^{n}(\gamma_i^2+\sigma_i^2)\bar{F}_2 = \sum_{i=1}^{n}(\gamma_i c_{\mathrm{eq},i}+\sigma_i k_{\mathrm{eq},i}) \end{cases} \tag{12}$$

Using the test points presented in Tab. 1 and applying them to Eqs. (12), one can obtain values for damping constant, friction force in the Freeplay region and in the damper. These results correspond to $C = 558.85$ N.s/m, $\bar{F}_1 = 14.154$ N, and $\bar{F}_2 = 68.424$ N.

The comparison of results obtained with the describing functions, represented by Eqs. (7) and (8), and those from tests are presented in Figs. 4 and 5.

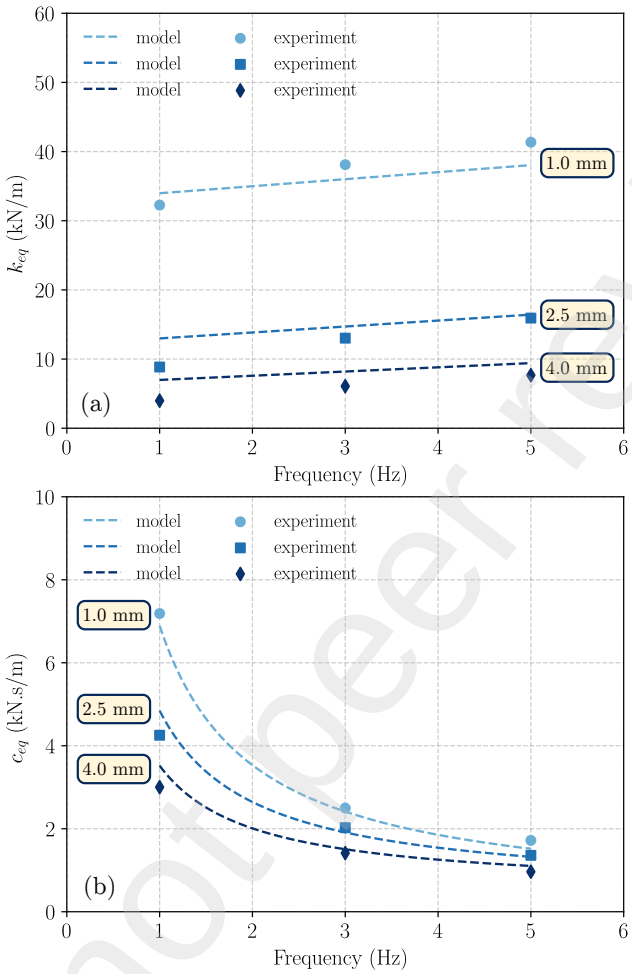

Figure 4: Comparison of the mathematical model and experimental results. (a) Equivalent stiffness for amplitudes A = 1.0, 2.5, 4.0 mm. (b) Equivalent damping for amplitudes A = 1.0, 2.5, 4.0 mm.

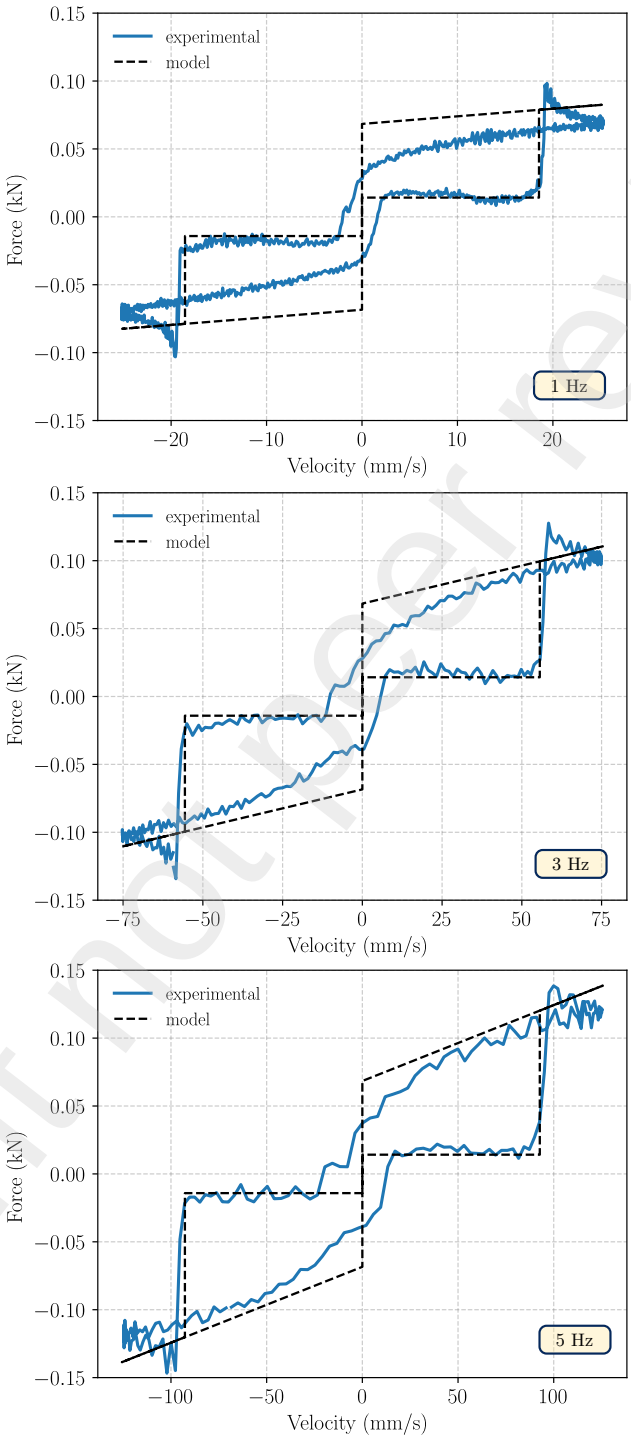

Figure 5: Experimental nonlinear behavior of the damper with Freeplay and friction.

The observation of Eqs. (7) and (8), and the results shown in Figs. 4 and 5 reveal that:

1. there is a stiffness-like term generated by the presence of a deadzone in the damping force and this is clearly shown in the experimental results; this equivalent stiffness is also predicted by the developed mathematical model;
2. the equivalent stiffness depends on the relative size of the deadzone with respect to the amplitude of motion; according to the developed mathematical model, this is shown as an inclination of a line representing the equivalent stiffness, for a certain amplitude, with respect to the frequency axis; the experimental results are consistent with this behavior;
3. the position where the straight line representing the equivalent stiffness intercepts the ordinates-axis (stiffness for zero frequency) depends on friction forces $\bar{F}_1$ and $\bar{F}_2$ and also on the amplitude A of the motion; again, the experimental data also show this behavior;
4. experimental data for the equivalent damping show that the behavior is typical of friction damping, tending to higher values for lower frequencies; this behavior agrees with the assumption of friction damping;
5. for higher frequencies, the experimental damping seems to approach a limit value which depends on the amplitude of the motion; this behavior agrees with the one predicted by the present mathematical model;
6. the results obtained with the present mathematical model, and consequently based on the idealization shown in Figs. 2(b) and 2(c), agree in a satisfactory manner with the experimental data, as shown in Figs. 4 and 5.

Based on these results, it is clear that the equivalent damping for the damper with friction and Freeplay can be predicted both qualitatively and quantitatively by the mathematical model under evaluation in this work. Is is easy to understand, observing Fig. 4, that the inclinations of the straight lines that represent the stiffness of the combination damper + friction + Freeplay agree in a satisfactory manner with those of the experimental data. The same happens with the part of damping that is invariant with frequency, depends on the linear damping coefficient C, and does not depend on friction forces $\bar{F}_1$ and $\bar{F}_2$. Friction, however, should be seen with some caution since it is a parameter with significant variation depending on the current conditions of the test. This variation of the friction force induces, as Eqs. (7) and

(8) predict, variations in the stiffness for zero frequency and in the part of damping that depends on the frequency.

Additionally, based on the experimental results shown in Fig. 5, it can be noticed that the damper used in this test is not perfectly linear outside the Freeplay zone. This characteristic could account for part of the differences between experimental results and mathematical predictions with the present model.

3.1. Comparison with Literature Results

Tong and Liebner [19] presented some experimental data for the energy dissipation loss of a damper with a deadzone that can be used for evaluation of the present describing functions. The Energy Dissipation Loss, R_{loss}, can be evaluated by using the describing function through the following equation:

$$R_{\text{loss}} = 1 - \frac{C_{\text{eq}}}{C} \tag{13}$$

In this case, to evaluate c_{eq}/c, the describing functions used were the ones in Eqs. (4) and (5), based on the model without friction represented in Fig. 2(c).

The results depicted in Figs. 6 show that the present mathematical model is in close agreement with the analytical results of Tong and Liebner [19]. Furthermore, the present results are close to the experimental data shown in Ref. [19] and referred to as actual data.

4. Conclusions

The present work presents an idealized mathematical model to represent the nonlinear behavior of a damper in combination with Freeplay. This damper may contain friction or not. One of the objectives of this research effort was to verify the validity of such a mathematical model by means of a comparison with experimental data.

The comparison of the results from the ground tests with the mathematical model represented by Eqs. (7) and (8) reveals that the idealized model for describing the behavior of a combination of damper with Freeplay is capable of obtaining satisfactory and consistent predictions when compared to experimental data.

In summary, the described functions obtained in this work can be used for the prediction of the behavior of nonlinear mechanical systems containing

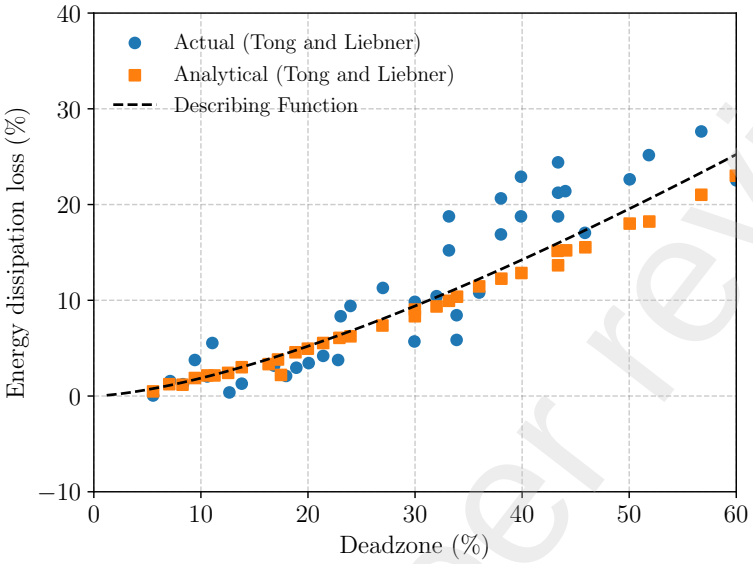

Figure 6: Comparison of Energy Dissipation loss using the describing function and the results given in [19] for different values of the deadzone.

a damper with a certain amount of deadspace. Moreover, the idealization used in the model is suitable for time domain simulations, since the Freeplay deadzone is characterized by its length.

Appendix A. Fourier Series and Describing Function

The Fourier series is commonly used in the analysis of periodic signals. Any periodic function $f(t)$ with period T can be represented by a sum of sines and cosines (or equivalently, exponentials) as [23]:

$$f(t) = a_0 + \sum_{n=1}^{\infty} \left(a_n \cos(n\omega_0 t) + b_n \sin(n\omega_0 t)\right) \tag{A.1}$$

where $\omega = \frac{2\pi}{T}$ is the fundamental frequency, and the Fourier coefficients are given by:

$$a_0 = \frac{1}{T} \int_0^T f(t)\, dt, \tag{A.2}$$

$$a_n = \frac{2}{T}\int_0^T f(t)\cos(n\omega t)\,dt, \tag{A.3}$$

$$b_n = \frac{2}{T}\int_0^T f(t)\sin(n\omega t)\,dt. \tag{A.4}$$

For systems with nonlinearities, the describing function is an approximate method that uses the Fourier series to characterize the response of a nonlinear element to a sinusoidal input. If the nonlinearity can be expressed as a function of the input amplitude A, the describing function $N(A)$ is defined as the ratio of the fundamental harmonic of the output to the input sinusoid:

$$N(A) = \frac{\text{Fundamental component of the output}}{A\sin(\omega t)}. \tag{A.5}$$

To obtain the describing function, the output of the nonlinear element is expanded into a Fourier series. Typically, only the first harmonic is considered for the describing function:

$$N(A) = \frac{1}{A\pi}\int_0^{2\pi} f(A\sin\theta)\sin\theta\,d\theta, \tag{A.6}$$

where $f(A\sin\theta)$ is the nonlinear function.

This method is commonly used in the analysis of systems with certain types of nonlinearities, such as saturation, dead zones, or hysteresis, to predict oscillatory behavior or limit cycles.

Appendix A.1. Describing function for a spring with Freeplay

Assuming $x(t) = A\sin(\omega t) = A\sin\theta$:

$$F(\theta) = \begin{cases} 0 & \text{for } \ 0 \le \theta < \theta_1 \\ k(x-\delta) = k(A\sin\theta - \delta) & \text{for } \ \theta_1 \le \theta < \pi - \theta_1 \\ 0 & \text{for } \ \pi - \theta_1 \le \theta < \pi + \theta_1 \\ k(x+\delta) = k(A\sin\theta + \delta) & \text{for } \ \pi + \theta_1 \le \theta < 2\pi - \theta_1 \\ 0 & \text{for } \ 2\pi - \theta_1 \le \theta < 2\pi \end{cases} \tag{A.7}$$

where:

$$\theta_1 = \arcsin\left(\frac{\delta}{A}\right)$$

All coefficients a_n are zero as $F(t)$ is an odd function.

$$b_1 = \frac{2}{\pi}\int_0^{\pi} F(\theta)\sin\theta\, d\theta = \frac{2}{\pi}\int_{\theta_1}^{\pi-\theta_1} k\left(A\sin\theta - \delta\right)\sin\theta\, d\theta \tag{A.8}$$

$$b_1 = \frac{2}{\pi}\left\{kA\int_{\theta_1}^{\pi-\theta_1}\sin^2\theta\, d\theta - k\delta\int_{\theta_1}^{\pi-\theta_1}\sin\theta\, d\theta\right\} \tag{A.9}$$

$$b_1 = \frac{2k}{\pi}\left\{A\left[\frac{\theta}{2} - \frac{\sin 2\theta}{4}\right]_{\theta_1}^{\pi-\theta_1} + \delta\left[\cos\theta\right]_{\theta_1}^{\pi-\theta_1}\right\} \tag{A.10}$$

$$b_1 = \frac{2k}{\pi}\left\{A\left[\frac{\pi}{2} - \theta_1 + \frac{\sin 2\theta_1}{2}\right] + \delta\left[-2\cos\theta_1\right]\right\} \tag{A.11}$$

$$b_1 = \frac{2k}{\pi}\left\{A\left[\frac{\pi}{2} - \theta_1 + \frac{\sin 2\theta_1}{2}\right] + \delta\left[-2\cos\theta_1\right]\right\} \tag{A.12}$$

$$b_1 = \frac{2k}{\pi}A\left\{\left[\frac{\pi}{2} - \theta_1 + \sin\theta_1\cos\theta_1\right] - 2\frac{\delta}{A}\cos\theta_1\right\} \tag{A.13}$$

$$b_1 = \frac{2}{\pi}kA\left\{\frac{\pi}{2} - \theta_1 + \frac{\delta}{A}\cos\theta_1 - 2\frac{\delta}{A}\cos\theta_1\right\} \tag{A.14}$$

$$b_1 = kA\frac{1}{\pi}\left\{\pi - 2\arcsin\left(\frac{\delta}{A}\right) - 2\left(\frac{\delta}{A}\right)\sqrt{1-\left(\frac{\delta}{A}\right)^2}\right\} \tag{A.15}$$

Finally,

$$F(t) \approx b_1\sin(\omega t) = k\left\{1 - \frac{2}{\pi}\arcsin\left(\frac{\delta}{A}\right) - \frac{2}{\pi}\left(\frac{\delta}{A}\right)\sqrt{1-\left(\frac{\delta}{A}\right)^2}\right\}A\sin(\omega t) \tag{A.16}$$

Knowing that $A\sin(\omega t) = x(t)$:

$$F(t) \approx k\left\{1 - \frac{2}{\pi}\arcsin\left(\frac{\delta}{A}\right) - \frac{2}{\pi}\left(\frac{\delta}{A}\right)\sqrt{1-\left(\frac{\delta}{A}\right)^2}\right\}x(t) \tag{A.17}$$

And then, by inspecton:

$$k_{\text{eq}} \approx k\left[1 - \frac{2}{\pi}\arcsin\left(\frac{\delta}{A}\right) - \frac{2}{\pi}\left(\frac{\delta}{A}\right)\sqrt{1-\left(\frac{\delta}{A}\right)^2}\right] \tag{A.18}$$

Appendix A.2. Describing function for a damper with Freeplay and Coulomb friction

Assuming $x(t) = A\sin(\omega t) = A\sin\theta$ and a linear damping outside the freeplay zone ($F = C\dot{x}$) and Coulomb friction both inside the damper ($F = \pm F_2$) and in the freeplay deadzone ($F = \pm F_1$):

$$F(\theta) = \begin{cases} C\dot{x} + F_2 = C\omega A\cos\theta + F_2 & \text{for } 0 \le \theta < \pi/2 \\ -F_1 & \text{for } \pi/2 \le \theta < \pi/2 + \theta_1 \\ C\dot{x} - F_2 = C\omega A\cos\theta - F_2 & \text{for } \pi/2 + \theta_1 \le \theta < 3\pi/2 \\ +F_1 & \text{for } 3\pi/2 \le \theta < 3\pi/2 + \theta_1 \\ C\dot{x} + F_2 = C\omega A\cos\theta + F_2 & \text{for } 3\pi/2 + \theta_1 \le \theta < 2\pi \end{cases} \tag{A.19}$$

where:

$$\theta_1 = \arccos\left(1 - \frac{2\delta}{A}\right)$$

Similarly to case 1, the nonlinear force represented by Eq. (A.19) may be expanded in a Fourier series and truncated in the first harmonics. Then:

$$a_1 = \frac{C\omega A}{\pi}\left(\pi - \theta_1 + \sin\theta_1\cos\theta_1\right) + \frac{2}{\pi}(F_1 + F_2) + \frac{2}{\pi}(F_2 - F_1)\cos\theta_1 \tag{A.20}$$

$$b_1 = \frac{C\omega A}{\pi}(1 - \cos^2\theta_1) + \frac{2}{\pi}(F_2 - F_1)\sin\theta_1 \tag{A.21}$$

The approximation of the nonlinear force can be written as:

$$\begin{aligned} F(t) &\approx a_1\cos(\omega t) + b_1\sin(\omega t) \\ &= \left[\tfrac{C\omega A}{\pi}\left(\pi - \theta_1 + \sin\theta_1\cos\theta_1\right) + \frac{2}{\pi}(F_1 + F_2) + \frac{2}{\pi}(F_2 - F_1)\cos\theta_1\right]\cos(\omega t) \\ &\quad + \left[\tfrac{C\omega A}{\pi}(1 - \cos^2\theta_1) + \frac{2}{\pi}(F_2 - F_1)\sin\theta_1\right]\sin(\omega t) \end{aligned} \tag{A.22}$$

This approximation can be rewritten as:

$$\begin{aligned} F(t) &\approx \left[\tfrac{C}{\pi}\left(\pi - \theta_1 + \sin\theta_1\cos\theta_1\right) + \frac{2}{\pi\omega A}(F_1 + F_2) + \frac{2}{\pi\omega A}(F_2 - F_1)\cos\theta_1\right]\dot{x}(t) \\ &\quad + \left[\tfrac{C\omega}{\pi}(1 - \cos^2\theta_1) + \frac{2}{\pi A}(F_2 - F_1)\sin\theta_1\right]x(t) \end{aligned} \tag{A.23}$$

Then, making the necessary substitutions and identifying that this force has a component in phase with the displacement and another in phase with the velocity:

$$c_{\text{eq}} = \frac{C}{\pi}\left[\pi - \arccos\left(1-\frac{2\delta}{A}\right) + \left(1-\frac{2\delta}{A}\right)\sqrt{1-\left(1-\frac{2\delta}{A}\right)^2}\right] + \frac{2}{\pi\omega A}(F_1+F_2) + \frac{2}{\pi\omega A}(F_2-F_1)\left(1-\frac{2\delta}{A}\right) \tag{A.24}$$

$$k_{\text{eq}} = \frac{C\omega}{\pi}\left[1-\left(1-\frac{2\delta}{A}\right)^2\right] + \frac{2}{\pi A}(F_2-F_1)\sqrt{1-\left(1-\frac{2\delta}{A}\right)^2} \tag{A.25}$$

References

[1] D. S. Woolston, H. L. Runyan, T. A. Byrdsong, Some effects of system nonlinearities in the problem of aircraft flutter, Technical Note 3539, National Advisory Committee for Aeronautics (NACA), USA, Langley Aeronautical Laboratory, Washington (Oct. 1955).

[2] D. Tang, E. H. Dowell, Experimental and theoretical study of gust response for a wing–store model with freeplay, Journal of Sound and Vibration 295 (3) (2006) 659–684. doi:10.1016/j.jsv.2006.01.024.

[3] H. Li, K. Ekici, Revisiting the one-shot method for modeling limit cycle oscillations: Extension to two-degree-of-freedom systems, Aerospace Science and Technology 69 (2017) 686–699. doi:10.1016/j.ast.2017.07.037.

[4] J. A. I. Silva, D. D. Bueno, G. L. C. M. Abreu, A strategy to suppress limit cycle oscillations in helicopter ground resonance including landing gear nonlinearities, Aerospace Science and Technology 105 (2020) 106011. doi:10.1016/j.ast.2020.106011.

[5] M. Dardel, F. Bakhtiari-Nejad, Limit cycle oscillation control of wing with static output feedback control method, Aerospace Science and Technology 24 (1) (2013) 147–160, vFE-2. doi:10.1016/j.ast.2011.08.013.

[6] N. Ramos-Pedroza, W. MacKunis, V. Golubev, A robust nonlinear output feedback control method for limit cycle oscillation suppression using synthetic jet actuators, Aerospace Science and Technology 64 (2017) 16–23. doi:10.1016/j.ast.2016.12.030.

[7] Z. Dimitrijević, G. D. Mortchéléwicz, F. Poirion, Nonlinear dynamics of a two dimensional airfoil with freeplay in an inviscid compressible flow, Aerospace Science and Technology 4 (2) (2000) 125–133. doi:10.1016/S1270-9638(00)00127-9.

[8] L. K. Abbas, Q. Chen, K. O'Donnell, D. Valentine, P. Marzocca, Numerical studies of a non-linear aeroelastic system with plunging and pitching freeplays in supersonic/hypersonic regimes, Aerospace Science and Technology 11 (5) (2007) 405–418. doi:10.1016/j.ast.2007.02.007.

[9] E. Atabay, I. Ozkol, Application of a magnetorheological damper modeled using the current–dependent bouc–wen model for shimmy suppression in a torsional nose landing gear with and without freeplay, Journal of Vibration and Control 20 (11) (2014) 1622–1644. doi:10.1177/1077546312468925.

[10] E. Verstraelen, G. Dimitriadis, G. D. B. Rossetto, E. H. Dowell, Two-domain and three-domain limit cycles in a typical aeroelastic system with freeplay in pitch, Journal of Fluids and Structures 69 (2017) 89–107. doi:https://doi.org/10.1016/j.jfluidstructs.2016.11.019.

[11] J. Panchal, H. Benaroya, Review of control surface freeplay, Progress in Aerospace Sciences 127 (2021) 100729. doi:10.1016/j.paerosci.2021.100729.

[12] D. A. Pereira, R. M. G. Vasconcellos, M. R. Hajj, F. D. Marques, Effects of combined hardening and free-play nonlinearities on the response of a typical aeroelastic section, Aerospace Science and Technology 50 (2016) 44–54. doi:10.1016/j.ast.2015.12.022.

[13] D. Eller, Friction, freeplay and flutter of manually controlled aircraft, in: IFASD - International Forum on Aeroelasticity and Structural Dynamics, 2007.

[14] L. D. Wayhs-Lopes, E. H. Dowell, D. D. Bueno, Influence of friction and asymmetric freeplay on the limit cycle oscillation in aeroelastic system: An extended hénon's technique to temporal integration, Journal of Fluids and Structures 96 (2020) 103054. doi:10.1016/j.jfluidstructs.2020.103054.

[15] D. B. Kholodar, Nature of freeplay-induced aeroelastic oscillations, Journal of Aircraft 51 (2) (2014) 571–583. arXiv:https://doi.org/10.2514/1.C032295, doi:10.2514/1.C032295.
URL https://doi.org/10.2514/1.C032295

[16] R. Adami, A. Teta, A simple model of concentrated nonlinearity, in: J. Dittrich, P. Exner, M. Tater (Eds.), Mathematical Results in Quantum Mechanics, Birkhäuser Basel, Basel, 1999, pp. 183–189. doi:10.1007/978-3-0348-8745-8_13.

[17] J. Den Hartog, Mechanical Vibrations, Civil, Mechanical and Other Engineering Series, Dover Publications, 1985.

[18] M. A. Padmanabhan, A theoretical and computational study of limit cycle oscillations in high performance aircraft, Ph.D. thesis, Duke University (2015).

[19] M. Tong, T. Liebner, Loss of energy dissipation capacity from the deadzone in linear and nonlinear viscous damping devices, Earthquake Engineering and Engineering Vibration 6 (2007) 11–20. doi:10.1007/s11803-007-0701-y.

[20] S. Huet, G. Broux, E. Garrigues, Aeroelastic behavior of a Falcon business jet in case of failed servo-actuator, in: 15th International Forum on Aeroelasticity and Structural Dynamics, 2011.

[21] D. D. Baker, Means of compliance with title 14 CFR, part 23, 23.629, flutter. Advisory Circular 23.629-1B. Federal Aviation Administration - FAA. U. S. Department of Transportation. (April 2004).

[22] K. Worden, G. Tomlinson, Nonlinearity in Structural Dynamics - Detection, Identification and Modelling, IOP Publishing Ltd, UK, 2001.

[23] W. E. Vander Velde, et al., Multiple-input describing functions and nonlinear system design, McGraw lill (1968).